Inorg. Chem. **2009**, *48*, 476−487

Aqueous V(V)-Peroxo-Amino Acid Chemistry. Synthesis, Structural and Spectroscopic Characterization of Unusual Ternary Dinuclear Tetraperoxo Vanadium(V)-Glycine Complexes

C. Gabriel,[†] M. Kaliva,[‡] J. Venetis,[†] P. Baran,[§,⊥] I. Rodriguez-Escudero,[§] G. Voyiatzis,[#] M. Zervou,[▽] and A. Salifoglou*[,†]

Laboratory of Inorganic Chemistry, Department of Chemical Engineering, Aristotle University of Thessaloniki, Thessaloniki 54124, Greece, Department of Chemistry, University of Crete, Heraklion 71409, Greece, Department of Chemistry, University of Puerto Rico, San Juan, Puerto Rico 00931-3346, Foundation for Research and Technology Hellas (FORTH), Institute of Chemical Engineering and High Temperature Chemical Processes (ICE/HT), Patras 26500, Greece, and Laboratory of Molecular Analysis, Institute of Organic and Pharmaceutical Chemistry, National Hellenic Research Foundation, Athens 11635, Greece

Received July 30, 2008

Vanadium participation in cellular events entails in-depth comprehension of its soluble and bioavailable forms bearing physiological ligands in aqueous distributions of binary and ternary systems. Poised to understand the ternary V(V)-H_2O_2-amino acid interactions relevant to that metal ion's biological role, we have launched synthetic efforts involving the physiological ligands glycine and H_2O_2. In a pH-specific fashion, V_2O_5, glycine, and H_2O_2 reacted and afforded the unusual complexes $(H_3O)_2[V_2(O)_2(\mu_2{:}\eta^2{:}\eta^1\text{-}O_2)_2(\eta^2\text{-}O_2)_2(C_2H_5NO_2)]\cdot 5/4H_2O$ (**1**) and $K_2[V_2(O)_2(\mu_2{:}\eta^2{:}\eta^1\text{-}O_2)_2(\eta^2\text{-}O_2)_2(C_2H_5NO_2)]\cdot H_2O$ (**2**). **1** crystallizes in the triclinic space group $P\bar{1}$, with $a = 7.805(4)$ Å, $b = 8.134(5)$ Å, $c = 12.010(7)$ Å, $\alpha = 72.298(9)°$, $\beta = 72.991(9)°$, $\gamma = 64.111(9)°$, $V = 641.9(6)$ Å^3, and $Z = 2$. **2** crystallizes in the triclinic space group $P\bar{1}$, with $a = 7.6766(9)$ Å, $b = 7.9534(9)$ Å, $c = 11.7494(13)$ Å, $\alpha = 71.768(2)°$, $\beta = 73.233(2)°$, $\gamma = 65.660(2)°$, $V = 610.15(12)$ Å^3, and $Z = 2$. Both complexes **1** and **2** were characterized by UV/visible, LC-MS, FT-IR, Raman, NMR spectroscopy, cyclic voltammetry, and X-ray crystallography. The structures of **1** and **2** reveal the presence of unusual ternary dinuclear vanadium-tetraperoxo-glycine complexes containing $[(V^V{=}O)(O_2)_2]^-$ units interacting through long V−O bonds and an effective glycinate bridge. The latter ligand is present in the dianionic assembly as a bidentate moiety spanning both V(V) centers in a zwitterionic form. The collective physicochemical properties of the two ternary species **1** and **2** project the chemical role of the low molecular mass biosubstrate glycine in binding V(V)-diperoxo units, thereby stabilizing a dinuclear V(V)-tetraperoxo dianion. Structural comparisons of the anions in **1** and **2** with other known dinuclear V(V)-tetraperoxo binary anionic species provide insight into the chemical reactivity of V(V)-diperoxo species in key cellular events such as insulin mimesis and antitumorigenicity, potentially modulated by the presence of glycinate and hydrogen peroxide.

Introduction

Vanadium participation in diverse abiotic applications and biological systems has been amply established in the past years and spurred considerable research activities aimed at delineating its role and biological action.[1] To the degree that vanadium involvement influences metabolic processes key to the physiology of organisms, vanadium metallobiochemistry has been at the forefront of attention, featuring the nature of the active sites and the incipient biochemistry in metalloenzyme systems[2] such as nitrogenases[3] and haloperoxidases.[4−8] Apart from its direct participation in the active sites of metalloenzymes, vanadium as an inorganic cofactor has been shown to possess and promote bioactivities extending from antitumorigenicity[9] to mitogenicity,[10] inhibition of metabolic enzymes (i.e., phosphoglucomutases) and others.[11]

* To whom correspondence should be addressed. E-mail: salif@auth.gr. Phone: +30-2310-996-179. Fax: +30-2310-996-196.
[†] Aristotle University of Thessaloniki.
[‡] University of Crete.
[§] University of Puerto Rico.
[⊥] Present address: Department of Chemistry, Juniata College, Huntingdon, Pennsylvania 16652, U.S.A.
[#] Institute of Chemical Engineering and High Temperature Chemical Processes (ICE/HT).
[▽] National Hellenic Research Foundation.

10.1021/ic801427b CCC: $40.75
Published on Web 12/11/2008

A very essential effect, however, was found to emerge for vanadium, with this metal ion influencing glucose catabolizing processes linked to the heterogeneous syndrome of Diabetes mellitus through insulin mimesis.[12,13] To this end, a number of vanadium compounds and peroxo-vanadates have been shown to generate biological and biochemical responses[14] and rise as potential insulin-mimetic agents in the treatment of human diabetes.[15]

In its role as a metal ionic inducer of metabolic events in cellular physiology, vanadium reacts with physiological substrates of low, as well as high, molecular mass. Among the plethora of such potential ligands are small molecules including H_2O_2 and amino acids or amino acid containing macromolecules, that is, peptides and proteins. To this end, H_2O_2 reacts readily with V(V), forming a number of peroxo-vanadates, the nature of which depends on (a) the pH of the reaction medium and (b) the relative molar concentrations of the reaction reagents. These compounds have been shown to exhibit a wide variety of activities in vivo and in vitro, including antitumorigenesis, catalysis, and insulin mimesis. The extent to which these activities are promoted depends on the specific structural features of (a) the peroxo moieties surrounding V(V), (b) the structural properties of any potential heteroligands that seek V(V) binding, and (c) the reaction conditions under which the synthesis of such species is achieved.

Given that low molecular mass substrates available in biological fluids are potential targets for vanadium chemistry, amino acids are primary such ligands eliciting interactions from metal ions either in their free form or in the form of peptides, proteins, and enzymes. The ultimate activity of vanadium bearing more than one peroxide and attracting aminoacids in its coordination sphere could be understood through detailed information of the arising ternary V(V)-peroxo-aminoacid interactions and the associated speciation as a function of pH and molecular stoichiometry of the participants. Given the paucity of well-defined structurally characterized V(V)-amino acid species bearing more than one peroxo moiety bound to them and exhibiting biological activity, research efforts were launched in our laboratory targeting the chemical reactivity in the ternary V(V)-H_2O_2-glycine system. Herein, we describe the synthesis, isolation, spectroscopic and structural characterization of unusual ternary dinuclear V(V) tetraperoxo species bearing a single amino acid glycine in the zwitterionic form. The properties of such a species are discussed in terms of its structural features potentially affecting the chemical reactivity of V(V) metal ion in a biologically relevant setting.

Experimental Section

Materials and Methods. All experiments were carried out under aerobic conditions. Nanopure quality water was used for all reactions. V_2O_5, glycine, and H_2O_2 30% were purchased from Aldrich. Ammonia and potassium hydroxide were supplied by Fluka.

Physical Measurements. FT-Infrared spectra were recorded on a Thermo, Nicolet IR 200 FT-infrared spectrometer. UV/visible measurements were carried out on a Hitachi U2001 spectrophotometer, in the range from 190 to 1000 nm. A ThermoFinnigan Flash EA 1112 CHNS elemental analyzer was used for the simultaneous determination of carbon, hydrogen, and nitrogen (%). The analyzer is based on the dynamic flash combustion of the sample (at 1800 °C) followed by reduction, trapping, complete gas

(1) (a) Rehder, D. *Bioinorganic Vanadium Chemistry*; Wiley: New York, 2008. (b) Rehder, D. *Org. Biomol. Chem.* **2008**, *6*, 957–964. (c) Baran, E. J. *J. Inorg. Biochem.* **2000**, *80*, 1–10. (d) Zubieta, J. *Comments Inorg. Chem.* **1994**, *3*, 153–183. (e) Chen, Q.; Salta, J.; Zubieta, J. *Inorg. Chem.* **1993**, *32*, 4485–4486. (f) Rehder, D. *Angew. Chem., Int. Ed. Engl.* **1991**, *30*, 148–167.

(2) (a) Bayer, E., *Metal Ions in Biological Systems: Amavadin, the Vanadium Compound of Amanitae*; Sigel, H., Sigel, A., Eds.; Marcel Dekker, Inc.: New York, 1995; Vol. *31*, Chapter 12, pp 407−421. (b) Smith, M. J.; Ryan, D. E.; Nakanishi, K.; Frank, P.; Hodgson, K. O., *Metal Ions in Biological Systems: Vanadium in Ascidians and the Chemistry in Tunichromes*; Sigel, H., Sigel, A., Eds.; Marcel Dekker, Inc.: New York, 1995; Vol. *31*, Chapter 13, pp 423−490. (c) Fraústo da Silva, J. J. R. *Chemical Speciation and Bioavailability* **1989**, *1*, 139–150.

(3) Liang, J.; Madden, M.; Shah, V. K.; Burris, R. H. *Biochem.* **1990**, *29*, 8577–8581.

(4) (a) Weyand, M.; Hecht, H.; Kiess, M.; Liaud, M.; Vilter, H.; Schomburg, D. *J. Mol. Biol.* **1999**, *293*, 595–611. (b) Vilter, H. *Metal Ions in Biological Systems: Vanadium and its Role in Life*; Sigel, H., Sigel, A., Eds.; Marcel Dekker, Inc.: New York, 1995; Vol. *31*, Chapter 10, pp 325−362. (c) Butler, A. *Curr. Opin. Chem. Biol.* **1998**, *2*, 279–285.

(5) Butler, A. *Coord. Chem. Rev.* **1999**, *187*, 17; and references cited therein.

(6) Pecoraro, V.; Slebodnick, C.; Hamstra, B. *Vanadium Compounds: Chemistry Biochemistry and Therapeutic Applications*; Crans, D. C., Tracey, A., Eds.; ACS Symposium Series 711; American Chemical Society: Washington, DC, 1998; Chapter 12.

(7) Ligtenbarg, A. G. J.; Hage, R.; Feringa, B. L. *Coord. Chem. Rev.* **2003**, *237*, 89.

(8) Van Schijndel, J. W. P. M.; Vollenbroek, E. G. M.; Wever, R. *Biochim. Biophys. Acta* **1993**, *1161*, 249.

(9) (a) Djordjevic, C. *Metal Ions in Biological Systems: Antitumorigenic Activity of Vanadium Compounds*; Sigel, H., Sigel, A., Eds.; Marcel Dekker, Inc.: New York, 1995; Vol. *31*, Chapter 18, pp 595−616. (b) Köpf-Maier, P.; Köpf, H. *Metal Compounds in Cancer Therapy*; Fricker, S. P., Ed.; Chapman and Hall: London, 1994; pp 109−146. (c) Djordjevic, C.; Wampler, G. L. *J. Inorg. Biochem.* **1985**, *25*, 51–55.

(10) (a) Klarlund, J. K. *Cell* **1985**, *41*, 707–717. (b) Smith, J. B. *Proc. Natl. Acad. Sci. U.S.A.* **1983**, *80*, 6162–6167.

(11) (a) Walton, K. M.; Dixon, J. E. *Annu. Rev. Biochem.* **1993**, *62*, 101–120. (b) Lau, K.-H. W.; Farley, J. R.; Baylink, D. J. *Biochem. J.* **1989**, *257*, 23–36.

(12) (a) Brand, R. M.; Hamel, F. G. *Int. J. Pharm.* **1999**, *183*, 117–123. (b) Drake, P. G.; Posner, B. I. *Mol. Cell. Biochem.* **1998**, *182*, 79–89. (c) Drake, P. G.; Bevan, A. P.; Burgess, J. W.; Bergeron, J. J.; Posner, B. I. *Endocrinology* **1996**, *137*, 4960–4968. (d) Eriksson, J. W.; Lönnroth, P.; Posner, B. I.; Shaver, A.; Wesslau, C.; Smith, U. P. *Diabetologia* **1996**, *39*, 235–242. (e) Stankiewicz, P. J.; Tracey, A. S., *Metal Ions in Biological Systems: Stimulation of Enzyme Activity by Oxovanadium Complexes*; Sigel, H., Sigel, A., Eds.; Marcel Dekker, Inc: New York, 1995; Vol. *31*, Chapter 8, pp 249−285.

(13) (a) Sakurai, H.; Kojima, Y.; Yoshikawa, Y.; Kawabe, K.; Yasui, H. *Coord. Chem. Rev.* **2002**, *226*, 187–198. (b) Sasagawa, T.; Yoshikawa, Y.; Kawabe, K.; Sakurai, H.; Kojima, Y. *J. Inorg. Biochem.* **2002**, *88*, 108–112. (c) Kanamori, K.; Nishida, K.; Miyata, N.; Okamoto, K.; Miyoshi, Y.; Tamura, A.; Sakurai, H. *J. Inorg. Biochem.* **2001**, *86*, 649–656. (d) Takino, T.; Yasui, H.; Yoshitake, A.; Hamajima, Y.; Matsushita, R.; Takada, J.; Sakurai, H. *J. Biol. Inorg. Chem.* **2001**, *6*, 133–142. (e) Melchior, M.; Rettig, S. J.; Liboiron, B. D.; Thompson, K. H.; Yuen, V. G.; McNeill, J. H.; Orvig, C. *Inorg. Chem.* **2001**, *40*, 4686–4690. (f) Sun, Q.; Sekar, N.; Goldwaser, I.; Gershonov, E.; Fridkin, M.; Shechter, Y. *Am. J. Physiol.: Endocrinol. Metab.* **2000**, *279*, E403–E410. (g) Goldwaser, I.; Gefel, D.; Gershonov, E.; Fridkin, M.; Shechter, Y. *J. Inorg. Biochem.* **2000**, *80*, 21–25. (h) Woo, L. C.; Yuen, V. G.; Thompson, K. H.; McNeill, J. H.; Orvig, C. *J. Inorg. Biochem.* **1999**, *76*, 251–257.

(14) Crans, D. C.; Smee, J. J.; Gaidamauskas, E.; Yang, L. *Chem. Rev.* **2004**, *104*, 849.

(15) Thompson, K. H.; McNeill, J. H.; Orvig, C. *Chem. Rev.* **1999**, *99*, 2561.

chromatographic separation and detection of the products. The instrument is (a) fully automated and controlled by PC via the Eager 300 dedicated software, and (b) capable of handling solid, liquid, or gaseous substances.

Solid State NMR Spectroscopy. Solid state CP-MAS ^{13}C NMR spectra were obtained on a Varian 400 MHz spectrometer, operating at 100.53 MHz. In each case, a sufficient sample quantity was placed in a 3.2 mm rotor. A double resonance HX probe was used. The spinning rate was set at 12 kHz. The RAMP-CP pulse sequence of the VnmrJ library was applied, whereby the ^{13}C spin-lock amplitude is varied linearly during CP, while the ^{1}H spin-lock amplitude is kept constant. RAMP-CP eliminates the Hartmann−Hahn matching profile dependence from the MAS spinning rate and optimizes signal intensity.[16] The spectra were recorded with 1000 scans, using a 90° pulse width of 5.8 μs, a contact pulse of 2 ms, and a recycle delay of 5 s. The adamantane ($C_{10}H_{16}$) CH group was used as an external reference (38.54 ppm) to report the chemical shifts of ^{13}C resonance peaks.

Solution NMR Spectroscopy. Solution ^{1}H- and ^{13}C NMR experiments were carried out on a Bruker AC 300 MHz spectrometer at 25 °C. The sample concentration was approximately 0.02−0.10 M in analyte. The compound was dissolved in D_2O. The ^{13}C spectral width was 20000 Hz. Experimental data were processed using the WIN-NMR software. Chemical shifts (δ) are reported in ppm relative to D_2O resonance peak.

LC-MS Spectroscopy. The MS measurements were obtained on a Shimadzu liquid chromatograph mass spectrometer LCMS-2010 EV, with a mass detector equipped with an ESI interface. A silica 1003.5 UMRP HPLC column (4.6 × 150 mm) was used at 35 °C. The solution of the sample used was a mixture of methanol 80% and water 20%. The employed flow rate was 0.4 mL min^{-1}. Full scan analysis was performed in the mass range 50−800 *m/z*.

Raman Spectroscopy. A T-64000 triple spectrometer (Jobin−Yvon−Horiba) was used for the Raman spectroscopic measurements. The Raman spectra were excited with the linearly polarized 514.5 nm line of an air-cooled Ar^+ laser (Spectra-Physics 163-A42). A narrow-bandpass interference filter was used for the elimination of the laser plasma lines. The excitation beam was directed to the sample compartment of a properly modulated metallurgical microscope (Olympus BHSM-BH2). The microscope was used for the delivery of the excitation laser beam on the sample, and the collection of the backscattered light through a beamsplitter and the objective lens adapted to the aperture of the microscope. The focusing objective was a Long Working distance (8 mm) 50X/0.55 Olympus lens. The spectra were obtained using a 0.5 mW laser power on the specimen for a total integration time of 100 s. A viewing screen connected to the microscope offered good sample positioning and beam focusing, as well as direct surface inspection before and after laser delivery. An increased laser power always resulted in darkening of the sample on the laser focused area. Scattered radiation was launched on the slit of a double premonochromator in a subtractive configuration for the elastic Rayleigh scattering rejection and then the Raman photons were directed to the spectrograph, where they had been dispersed, and detected by a 1800-grooves/mm grating and a 2D CCD detector (operating at 140K), respectively. The spectral slit width was approximately 4 cm^{-1}. The Raman spectra were obtained without use of any polarizer, half-wave plate, or analyzer; however, a quarter wave plate was positioned either just after the laser or between the focusing long working distance objective and the sample. In the latter case, the preference of the different optics (i.e., of the beam splitter) to a certain polarization was avoided, and the wave vector of the electric field of the excitation line was almost perfectly circularly polarized, giving the opportunity to obtain spectra not sensitive to the polarization Raman.

Electrochemical Measurements. Cyclic voltammetric measurements were carried out with an Autolab model PGSTAT100 potentiostat-galvanostat. The entire system was under computer control and supported by the appropriate computer software Autolab software GPES, running on Windows. The electrochemical cell used had platinum (disk) working and auxiliary (wire) electrodes. As reference electrode, a saturated Ag/AgCl electrode was used. The water used in the electrochemical measurements was of nanopure quality. KNO_3 was used as a supporting electrolyte. Normal concentrations used were 1−6 mM in electroanalyte and 0.1 M in supporting electrolyte. Purified argon was used to purge the solutions prior to the electrochemical measurements. Derived $E_{1/2}$ values are reported versus Ag/AgCl electrode.

Preparation of Complex $(H_3O)_2[V_2(O)_2(\mu_2:\eta^2:\eta^1\text{-}O_2)_2(\eta^2\text{-}O_2)_2(C_2H_5NO_2)]\cdot 5/4H_2O$ (1). A sample of V_2O_5 (0.20 g, 1.1 mmol) was dissolved in 5 mL of H_2O, and a solution of aqueous ammonia (1.0 N) was added slowly under stirring. The resulting slurry was heated and stirred at 50 °C. After 2 h, glycine (0.70 g, 9.3 mmol) was added under continuous stirring. The reaction slurry remained white in color. Stirring continued for an additional hour at room temperature. Subsequently, HCl was added dropwise until the solution turned clear. The final pH of the solution was 4.5, and the color was yellow. The reaction flask was then placed on an ice bath, and hydrogen peroxide 30% (0.60 g, 18 mmol) was added slowly and under continuous stirring. The solution turned clear yellow-orange and stayed on as such. The reaction flask was placed at 4 °C, and ethanol was added. A few days later, yellow crystalline material precipitated and was isolated by filtration and dried in vacuo. Yield: 0.40 g (38%). Anal. Calcd for **1**, $(H_3O)_2[V_2(O)_2(\mu_2:\eta^2:\eta^1\text{-}O_2)_2(\eta^2\text{-}O_2)_2(C_2H_5NO_2)]\cdot 5/4H_2O$ (**1**). ($C_2H_{13.5}NO_{15.25}V_2$, MW = 397.52): Calcd: C, 6.04; H, 3.40; N, 3.52 Found: C, 5.98; H, 3.34; N, 3.46.

Preparation of Complex $K_2[V_2(O)_2(\mu_2:\eta^2:\eta^1\text{-}O_2)_2(\eta^2\text{-}O_2)_2(C_2H_5NO_2)]\cdot H_2O$ (2). A sample of V_2O_5 (0.20 g, 1.1 mmol) was dissolved in 5 mL of H_2O, and a solution of KOH was added slowly under stirring. The resulting slurry was heated and stirred at 50 °C for 2 h. Afterward, glycine (0.45 g, 6.0 mmol) was added under continuous stirring. Stirring continued for an additional hour at room temperature. Subsequently, HCl was added until the solution turned clear. The final pH of the solution was 5.5, and the color was yellow. The reaction flask was then placed on an ice bath, and hydrogen peroxide 30% (0.60 g, 18 mmol) was added slowly and under continuous stirring. The solution turned yellow-orange and stayed on as such. The reaction flask was placed at 4 °C, and ethanol was added. A few days later, yellow crystalline material precipitated. It was isolated by filtration and dried in vacuo. Yield: 0.30 g (30%). Anal. Calcd for **2**, $K_2[V_2(O)_2(\mu_2:\eta^2:\eta^1\text{-}O_2)_2(\eta^2\text{-}O_2)_2(C_2H_5NO_2)]\cdot H_2O$ (**2**). (LC-MS $[V_2(O)_2(O_2)_4(C_2H_5NO_2)]$ *m/z* 337.24, $[V_2(O)_2(O_2)_4H]$ *m/z* 263.11, $[V_2O_2(O_2)H]$ *m/z* 167.11, [Gly-H] = $[C_2H_4NO_2]$ *m/z* 74.04). ($C_2H_7NO_{13}K_2V_2$, MW=433.17): Calcd: C, 5.54; H, 1.62; N, 3.23 Found: C, 5.73; H, 1.68; N, 3.38.

X-ray Crystal Structure Determination. X-ray quality crystals of compounds **1** and **2** were grown from mixtures of water-ethanol solutions. A single crystal, with dimensions 0.14 × 0.09 × 0.07 mm (**1**) and 0.13 × 0.10 × 0.09 mm (**2**) was mounted on the tip of a glass fiber with epoxy glue. X-ray diffraction data were collected on a Bruker AXS SMART 1K CCD area detector, with graphite monochromated Mo Kα radiation (λ = 0.71073 Å), at

(16) Metz, G.; Wu, X. L.; Smith, S. O. *J. Magn. Reson., Ser. A* **1994**, *110*, 219–227.

Table 1. Summary of Crystal, Intensity Collection, and Refinement Data for $(H_3O)_2[V_2(O)_2(\mu_2{:}\eta^2{:}\eta^1\text{-}O_2)_2(\eta^2\text{-}O_2)_2(C_2H_5NO_2)]\cdot 5/4H_2O$ (**1**) and $K_2[V_2(O)_2(\mu_2{:}\eta^2{:}\eta^1\text{-}O_2)_2(\eta^2\text{-}O_2)_2(C_2H_5NO_2)]\cdot H_2O$ (**2**)

	1	**2**
formula	$C_2H_{13.5}NO_{15.25}V_2$	$C_2H_7NK_2O_{13}V_2$
formula weight	397.52	433.17
T, °K	300(2)	293(2)
wavelength, λ (Å)	0.71073	0.71073
space group	$P\bar{1}$	$P\bar{1}$
a (Å)	7.805(4)	7.6766(9)
b (Å)	8.134(5)	7.9534(9)
c (Å)	12.010(7)	11.7494(13)
α, deg	72.298(9)	71.768(2)
β, deg	72.991(9)	73.233(2)
γ, deg	64.111(9)	65.660(2)
V, (Å^3)	641.9 (6)	610.15(12)
Z	2	2
D_{calcd} (Mg m^{-3})	2.057	2.358
abs.coeff. (μ), mm^{-1}	1.541	2.285
range of h, k, l	−9→9, −7→10, −15→14	−8→10, −9→10, −15→15
goodness-of-fit on F^2	1.033	1.010
no. of parameters	191	182
R [a]	0.0392[b]	0.0517[b]
R_w [a]	0.1057[b]	0.1125[b]

[a] R values are based on F values, R_w values are based on F^2. $R = \sum||F_o| - |F_c||/\sum|F_o|$; $R_w = (\sum[w(F_o^2 - F_c^2)^2]/\sum w(F_o^2)^2)^{1/2}$, $w = 1/[\sigma^2(F_o^2) + (aP)^2 + bP]$ where $P = (\text{Max}\ (F_o^2,0) + 2F_c^2)/3$. [b] For 2707 (**1**) and 1910 (**2**) reflections with $I > 2\sigma(I)$.

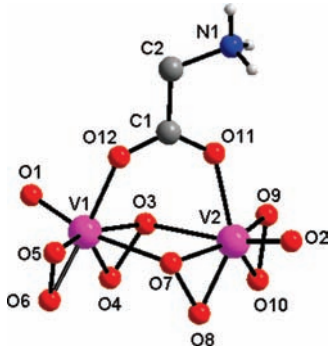

Figure 1. Crystal structure diagram of the $[V_2(O)_2(\mu_2{:}\eta^2{:}\eta^1\text{-}O_2)_2(\eta^2\text{-}O_2)_2(C_2H_5NO_2)]^{2-}$ anion with the atom labeling scheme in **1**.

room temperature using the program SMART-NT.[17] The collected data were processed by SAINT-NT.[18] An empirical absorption correction was applied by the program SADABS.[18] The structures were solved by direct methods and refined by full-matrix least-squares methods on F^2.[19] In both structures (**1** and **2**), all non-hydrogen atoms were refined anisotropically. Hydrogen atoms riding on carbon atoms were geometrically positioned and were left riding on their parent atoms during structure refinement. Hydrogen atom positions, which belong to oxygen atoms, were first determined from E-maps, brought to reasonable distances from their parent oxygen atoms, and then fixed. The final assignment satisfies the electroneutrality of compounds **1** and **2**, with the understanding that vanadium atoms are formally in the oxidation number +5. Crystallographic details for **1** and **2** are summarized in Table 1. Details on the crystallographic studies as well as atomic displacement parameters are given as Supporting Information in the form of cif files. Further experimental crystallographic details for **1**: $2\theta_{max}$ = 55.8°; number of reflections collected/unique/used, 3684/27707 [R(int) = 0.0164]/2255; 191 parameters refined; $(\Delta\rho)_{max}/(\Delta\rho)_{min}$ = 0.569/−0.545 e/Å^3; GOF = 1.169; R/R_w (for all data), 0.050/0.1057. Further experimental crystallographic details for **2**: $2\theta_{max}$ = 55.94°; number of reflections collected/unique/used, 5480/2803[R(int) = 0.0354]/1910; 182 parameters refined; $(\Delta\rho)_{max}/(\Delta\rho)_{min}$ = 1.022/−0.677 e/Å^3; GOF = 1.010; R/R_w (for all data), 0.0863/0.1230.

(17) *SMART-NT*, Version 5.0; Brucker AXS: Madison, WI, 1998.
(18) *SAINT-NT*, Version 5/6.0; Brucker AXS: Madison, WI, 1999.
(19) *SHELXTL-NT*, Version 5.1; Brucker AXS: Madison, WI, 1998.

Table 2. Bond Lengths [Å] and Angles [deg] for $(H_3O)_2[V_2(O)_2(\mu_2{:}\eta^2{:}\eta^1\text{-}O_2)_2(\eta^2\text{-}O_2)_2\ (C_2H_5NO_2)]\cdot 5/4H_2O$ (**1**) and $K_2[V_2(O)_2(\mu_2{:}\eta^2{:}\eta^1\text{-}O_2)_2(\eta^2\text{-}O_2)_2\ (C_2H_5NO_2)]\cdot H_2O$ (**2**)[a]

1		**2**	
	Bond Distances		
V(1)—O(12)	2.058(2)	V(1)—O(1)	2.056(3)
V(1)—O(5)	1.906(2)	V(1)—O(3)	1.891(3)
V(1)—O(6)	1.877(3)	V(1)—O(4)	1.865(3)
V(1)—O(3)	1.926(2)	V(1)—O(5)	1.938(3)
V(1)—O(4)	1.877(3)	V(1)—O(6)	1.894(3)
V(1)—O(1)	1.609(2)	V(1)—O(11)	1.609(3)
V(1)—O(7)	2.328(3)	V(1)—O(9)	2.379(3)
V(2)—O(11)	2.065(2)	V(2)—O(2)	2.047(3)
V(2)—O(9)	1.893(2)	V(2)—O(7)	1.911(3)
V(2)—O(10)	1.871(3)	V(2)—O(8)	1.869(3)
V(2)—O(7)	1.937(2)	V(2)—O(9)	1.929(3)
V(2)—O(8)	1.884(2)	V(2)—O(10)	1.885(3)
V(2)—O(2)	1.617(2)	V(2)—O(12)	1.609(3)
V(2)—O(3)	2.354(3)	V(2)—O(5)	2.346(3)
	Angles		
O(1)—V(1)—O(6)	104.52(11)	O(11)—V(1)—O(6)	99.00(16)
O(1)—V(1)—O(4)	101.70(12)	O(4)—V(1)—O(6)	89.14(15)
O(6)—V(1)—O(4)	88.50(11)	O(11)—V(1)—O(3)	100.48(16)
O(1)—V(1)—O(5)	102.13(12)	O(4)—V(1)—O(3)	45.92(14)
O(6)—V(1)—O(5)	45.56(11)	O(6)—V(1)—O(3)	134.15(15)
O(4)—V(1)—O(5)	132.25(11)	O(11)—V(1)—O(5)	102.70(15)
O(1)—V(1)—O(3)	102.15(11)	O(4)—V(1)—O(5)	129.66(15)
O(6)—V(1)—O(3)	130.36(11)	O(6)—V(1)—O(5)	44.87(13)
O(4)—V(1)—O(3)	45.19(9)	O(3)—V(1)—O(5)	156.51(14)
O(5)—V(1)—O(3)	155.30(11)	O(11)—V(1)—O(1)	94.42(15)
O(1)—V(1)—O(12)	91.96(11)	O(4)—V(1)—O(1)	130.97(14)
O(6)—V(1)—O(12)	131.97(11)	O(6)—V(1)—O(1)	132.65(13)
O(4)—V(1)—O(12)	132.36(10)	O(3)—V(1)—O(1)	86.53(14)
O(5)—V(1)—O(12)	87.25(11)	O(5)—V(1)—O(1)	87.93(13)
O(3)—V(1)—O(12)	87.47(10)	O(11)—V(1)—O(9)	170.09(15)
O(1)—V(1)—O(7)	166.54(11)	O(4)—V(1)— O(9)	84.15(13)
O(6)—V(1)—O(7)	86.24(9)	O(6)—V(1)— O(9)	86.58(12)
O(4)—V(1)—O(7)	86.41(9)	O(3)—V(1)— O(9)	81.05(13)
O(5)—V(1)—O(7)	79.47(9)	O(5)—V(1)— O(9)	75.46(12)
O(3)—V(1)—O(7)	75.86(8)	O(1)—V(1)— O(9)	75.85(11)
O(12)—V(1)—O(7)	74.72(8)	O(11)—V(1)—O(4)	104.01(16)
O(2)—V(2)—O(10)	104.30(11)	O(12)—V(2)—O(8)	104.57(17)
O(2)—V(2)—O(8)	99.48(11)	O(12)—V(2)—O(10)	102.03(17)
O(10)—V(2)—O(8)	88.38(10)	O(8)—V(2)—O(10)	88.45(15)
O(2)—V(2)—O(9)	100.07(12)	O(12)—V(2)—O(7)	103.24(17)
O(8)—V(2)—O(9)	133.48(11)	O(8)—V(2)—O(7)	45.39(14)
O(2)—V(2)—O(7)	103.10(11)	O(10)—V(2)—O(7)	131.58(16)
O(10)—V(2)—O(7)	129.01(11)	O(12)—V(2)—O(9)	101.99(16)
O(8)—V(2)—O(7)	45.03(9)	O(8)—V(2)—O(9)	130.46(15)
O(9)—V(2)—O(7)	156.58(11)	O(10)—V(2)—O(9)	45.18(13)
O(2)—V(2)—O(11)	93.76(11)	O(7)—V(2)—O(9)	154.36(14)
O(10)—V(2)—O(11)	130.79(10)	O(12)—V(2)—O(2)	91.32(16)
O(8)—V(2)—O(11)	133.66(9)	O(8)—V(2)—O(2)	131.63(15)
O(9)—V(2)—O(11)	86.39(10)	O(10)—V(2)—O(2)	133.01(13)
O(7)—V(2)—O(11)	88.76(10)	O(7)—V(2)—O(2)	86.78(14)
O(2)—V(2)—O(3)	169.05(10)	O(9)—V(2)—O(2)	88.14(13)
O(10)—V(2)—O(3)	84.68(9)	O(12)—V(2)—O(5)	165.55(15)
O(8)—V(2)—O(3)	86.84(9)	O(8)—V(2)—O(5)	86.66(13)
O(9)—V(2)—O(3)	81.57(9)	O(10)—V(2)—O(5)	87.10(14)
O(7)—V(2)—O(3)	75.04(9)	O(7)—V(2)—O(5)	78.00(13)
O(11)—V(2)—O(3)	75.49(8)	O(9)—V(2)—O(5)	76.42(12)
O(10)—V(2)—O(9)	45.89(10)	O(2)—V(2)—O(5)	74.32(12)

[a] Symmetry transformations used to generate equivalent atoms. (**1**) (i) 1 − x, 1 − y, 2 − z. (**2**) (i) −x, 2 − y, −z; (ii) −x, 1 − y, −z; (iii) −1 + x, y, z; (iv) −1 − x, 2 − y, −z; (v) −x, 1 − y, 1 − z; (vi) 1 − x, 1 − y, 1 − z; (vii) 1 + x, y, z.

Results

Synthesis. The synthetic exploration of the ternary V(V)-peroxo-glycine system led to the $(H_3O)_2[V_2(O)_2(\mu_2{:}\eta^2{:}\eta^1\text{-}O_2)_2(\eta^2\text{-}O_2)_2(C_2H_5NO_2)]\cdot 5/4H_2O$ (**1**) complex through a facile reaction among simple reagents in aqueous solutions. In a typical reaction, V_2O_5 reacted with glycine in the presence of aqueous ammonia at pH 4.5. Addition of dilute hydrogen peroxide solution (vide infra) promoted efficiently the peroxidation reaction of vanadium. The overall stoichiometric reaction leading to complex **1** is shown schematically below:

$$V_2O_5 + C_2H_5NO_2 + 4H_2O_2 \xrightarrow{\text{pH} \sim 4.5} (H_3O)_2[V_2(O)_2(\mu_2{:}\eta^2{:}\eta^1\text{-}O_2)_2(\eta^2\text{-}O_2)_2(C_2H_5NO_2)] + H_2O \quad (1)$$

In a similar reaction, V_2O_5 reacted initially with glycine in the presence of aqueous KOH, followed by addition of HCl and hydrogen peroxide at pH 5.5. Potassium hydroxide was important for two reasons. It helped adjust the pH of the reaction medium, at which the specific synthesis was carried out, and at the same time provided the cations necessary for balancing the negative charge on the derived anionic complex. The stoichiometric reaction leading to the formation of the compound $K_2[V_2(O)_2(\mu_2{:}\eta^2{:}\eta^1\text{-}O_2)_2(\eta^2\text{-}O_2)_2(C_2H_5NO_2)]\cdot H_2O$ (**2**) is shown below:

$$V_2O_5 + C_2H_5NO_2 + 4H_2O_2 + 2KOH \xrightarrow{\text{pH} \sim 5.5} K_2[V_2(O)_2(\mu_2{:}\eta^2{:}\eta^1\text{-}O_2)_2(\eta^2\text{-}O_2)_2(C_2H_5NO_2)] + 5H_2O \quad (2)$$

Ethanol, added as a precipitating solvent to the reaction mixture in both reactions described above, afforded yellow crystalline materials, the analytical composition of which was consistent with the formulation in **1** and **2** respectively (vide supra). Positive identification of the crystalline products was achieved by spectroscopic methods and X-ray crystallography for one of the isolated single crystals from **1** and **2**. Both complexes are stable, in the crystalline form, in the air, for fairly long periods of time. Both species are readily soluble in water and insoluble in dimethyl sulfoxide (DMSO), *N*,*N*′-dimethylformamide (DMF), acetonitrile, alcohols (CH_3OH, *i*-PrOH), and dichloromethane at room temperature even after heating up of the respective solutions. Aqueous solutions of both species are stable for over 24 h, beyond which time the compounds start slowly to lose peroxide as attested to by UV−visible spectroscopy. The LC-MS spectrum of **2** showed the presence of the intact anionic complex, thus confirming its integrity in solution and consistence with the structure displayed in the solid state.

Description of X-ray Crystallographic Structures. The X-ray crystal structures of **1** and **2** consist of discrete anions and cations in the respective lattices. Both complexes **1** and **2** crystallize in the triclinic space group $P\bar{1}$ with two molecules in the unit cell. The crystal structure diagram of the anion in **1** is shown in Figure 1 (the anion in **2** is provided as Supporting Information). A list of selected bond distances and angles for **1** and **2** are given in Table 2. The anionic assembly in both complexes is a dinuclear species consisting of two V(V) ions. Each V(V) is coordinated to two O_2^{2-} peroxide groups (O(3)−O(4), O(5)−O(6) for V(1) and O(7)−O(8), O(9)−O(10) for V(2) in **1** and **2**) and one doubly bonded oxo group (O(1) for V(1) and O(2) for V(2) in **1**, and O(11) for V(1) and O(12) for V2 in **2**). Each peroxo group binds V(V) in a side-on fashion, thus occupying two coordination sites around the metal ion center. One of the two V(V)-bound peroxo groups utilizes one of its two oxygens (O(3) and O(7) in **1**, and O(5) and O(9) in **2**, respectively) to span over to the second V(V) center, thus acting as a bridge and promoting a dinuclear assembly. The fifth coordination site around each V(V) ion is taken up by one of the oxygen terminals (O(12) for V(1) and O(11) for V(2) in **1**, and O(1) for V(1) and O(2) for V(2) in **2**) of the carboxylate group belonging to the amino acid ligand glycine. Therefore, the two peroxide ligands attached to each V(V) ion along with one oxygen terminal from the carboxylate group of glycinate lie in the equatorial plane, while the doubly bonded oxygen along with one of the oxygens of the peroxo group belonging to the adjacently located V(V) center occupy the axial positions (O(1), O(7) for V(1) and O(2), O(3) for V(2) in **1**, and O(11), O(9) for V(1) and O(12), O(5) for V(2) in **2**) of the pentagonal bipyramid around each V(V) center.

The carboxylic group of the glycine ligand is deprotonated while the amine group is protonated. To this end, the glycine ligand acts as a zwitterion with an overall zero charge. The overall charge of the dinuclear complex assembly is 2−. In the case of complex **1**, the counterion for balancing the negative charge is $[H_3O]^+$, whereas in the case of complex **2** the counterion is K^+.

The V−O bond distances in **1** (1.871(3)−2.354(3) Å) and **2** (1.865(3)−2.379(3) Å) are similar to the corresponding distances in other V(V)-diperoxo species such as $(Hbipy)[H\{VO(O_2)_2(bipy)\}_2]\cdot xH_2O_2\cdot(6-x)H_2O$ ($x\sim0.5$) (1.875(3)−2.480(2)Å),[20] $(NH_4)_4[O\{VO(O_2)_2\}_2]$(1.875(3)−2.522(3) Å),[21] $(NH_4)_4[V_2O_{11}]$ (1.839(18)−2.531(18) Å),[22] $[N(CH_3)_4]_2[V_2O_2(O_2)_4(H_2O)]\cdot 2H_2O$ (1.863(4)−2.045(3) Å),[23] $CymH_2[V_2O_2(O_2)_4(H_2O)]\cdot 2H_2O$ (1.868(4)−2.035(4) Å),[24] and V(V)-peroxo-carboxylate containing dinuclear complexes, such as $(NH_4)_6[V_2O_2(O_2)_2(C_6H_4O_7)_2]\cdot 4.5H_2O$ (1.894(3)−2.322(3) Å),[25] $(NH_4)_2[V_2O_2(O_2)_2(C_6H_6O_7)_2]\cdot 2H_2O$ (1.873(2)−2.034(2) Å),[26] $K_2[V_2O_2(O_2)_2(C_6H_6O_7)_2]\cdot 2H_2O$ (1.873(1)−2.039(1) Å),[27] $(NH_4)_4[V_2O_2(O_2)_2(C_4H_3O_5)_2]\cdot 3H_2O$ (1.859(3)−2.294(3) Å),[28] $K_4[V_2O_2(O_2)_2(C_4H_3O_5)_2]\cdot 4H_2O$ (1.868(2)−2.248(2) Å),[28] $K_2[V_2O_2(O_2)_2(C_4H_4O_5)_2]\cdot 2H_2O$ (1.869(2)−2.033(2) Å).[28] The V=O bond distances (1.609(2)−1.617(2) (**1**) and 1.609(3) (**2**)) are similar to those in the congener complex $(NH_4)_6[V_2O_2(O_2)_2(C_6H_4O_7)_2]\cdot 4.5H_2O$ (1.597(3) Å),[25] and similar to the calculated average value of 1.609(7) Å for over eleven V(V)-peroxo structures.[29] The angles in complex **1** are similar to those observed in a number of $V^V(=O)(O_2)_x$ ($x = 1, 2$) and $V^V{}_2O_2$ core-containing dimers, exhibiting distorted pentagonal bipyramidal geometry of the bound hydroxycarboxylate citrates around the vanadium(V) ions.[25−27]

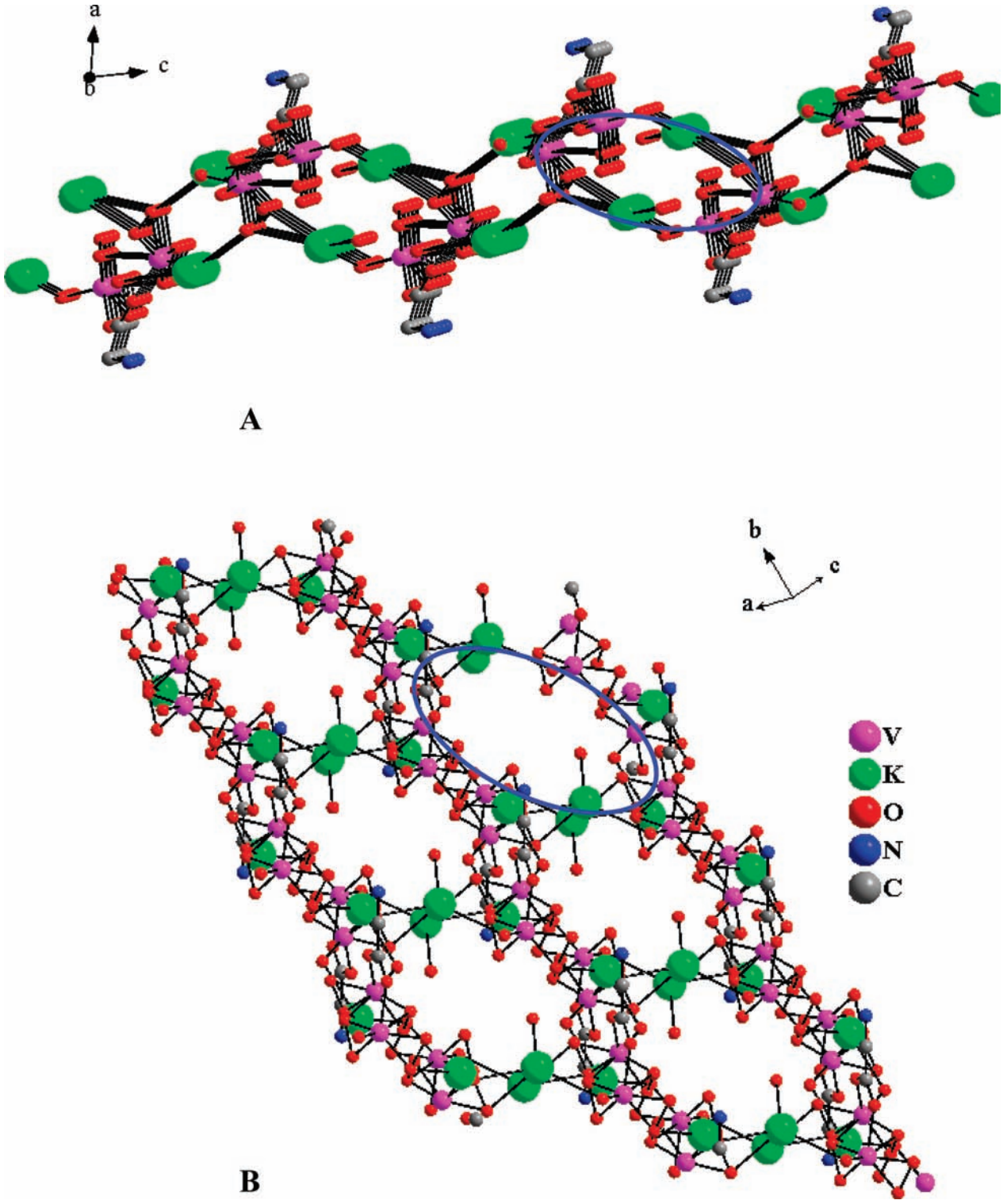

Figure 2. Packing diagram of **2** in the *ac* plane (**A**), and along the *abc* diagonal (**B**).

In complex **1**, the H_3O^+ counterions are sufficient in counteracting the charge generated by the dinuclear vanadium assembly. In complex **2**, the counterions are potassium ions. The potassium ions K(1) and K(2) show contact interactions with nine oxygen atoms in the range 2.696(4)−3.243(4) Å (K(1)) and 2.667(5)−3.249(7) Å (K(2)). These interactions include surrounding oxygens belonging to (a) oxygen atoms of peroxide ligands bound to both $[(V{=}O)(O_2)_2]^-$ units of the dinuclear tetraperoxo assembly, and (b) oxygen atoms doubly bonded to both vanadium centers of the dinuclear assembly. Hence, the potassium counterions are positioned in the lattice so as to optimally interact with the anions in **2**, providing neutralization of the generated 2− charge and incipient lattice stabilization (Figure 2). The existence of H_3O^+ ions in **1** and water molecules of crystallization in both **1** and **2** contribute to the stability of the respective lattice through hydrogen bond formation.

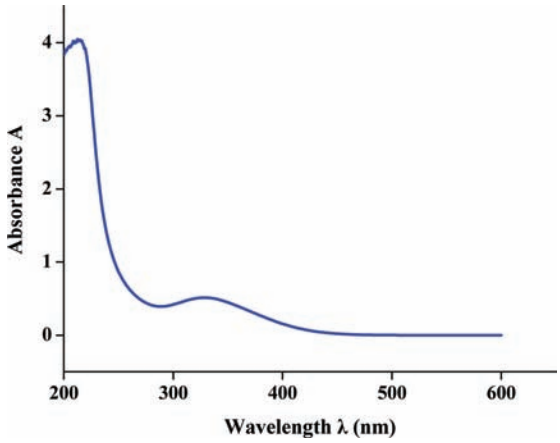

Figure 3. UV−visible spectrum of **1** in water.

UV/Visible Spectroscopy. The electronic spectrum of **1** was recorded in H_2O (Figure 3). The spectrum showed a band at 328 nm ($\varepsilon = 541\ M^{-1}\ cm^{-1}$) with a rising absorbance into the ultraviolet region. An additional feature was observed at around 213 nm ($\varepsilon = 4257\ M^{-1}\ cm^{-1}$). The spectrum was featureless beyond 400 nm. The band at 328 nm has been attributed to the presence of a peroxo to vanadium Ligand to Metal Charge Transfer (LMCT).[30] It appears, therefore, that at the pH examined here, the peroxo groups remain attached to the vanadium ion, further supporting the idea of a stable $[(V{=}O)(O_2)_2]^-$ unit in both complexes. The presence of the weak LMCT band, as suggested by Evans,[31] was also observed in other vanadium-peroxo complexes and was reasonably attributed to a $\pi_v^* \rightarrow d\sigma^*$ transition.[30] The intense absorption band at 213 nm in **1**, in the ultraviolet region, may be associated with a $(\sigma)\pi_v^* \rightarrow d\sigma^*$ LMCT transition. This transition had been previously proposed to occur at energies higher than that expected because of the $\pi^* \rightarrow$ d transition.[32] Further definitive assignments are difficult to make at the present time in the absence of detailed spectroscopic studies.[30,32]

FT-IR Spectroscopy. The Fourier transform (FT)-Infrared spectra of **1** and **2** were recorded in KBr and reflected the presence of vibrationally active carboxylate groups. Antisymmetric and symmetric vibrations for the carboxylate groups of the coordinated glycine ligands were observed in both cases. Specifically, the antisymmetric stretching vibrations $\nu_{as}(COO^-)$ for the carboxylate carbonyl emerged in the range 1620−1572 cm^{-1} for **1** and 1648−1509 cm^{-1} for **2**. Symmetric stretching vibrations $\nu_s(COO^-)$ for the same group appeared in the range 1412−1342 cm^{-1} for **1** and 1412−1287 cm^{-1} for **2**. The observed carbonyl vibrations were shifted to lower frequency values in comparison to the corresponding vibrations in free glycine, suggesting changes in the vibrational status of the glycinate ligand bound to vanadium.[33] The latter indication was attested to by the X-ray crystal structures of **1** and **2**. Furthermore, the $\nu(O\cdots O)$ vibration appeared at 878 cm^{-1} for both **1** and **2**, while the $\nu(VO)$ vibration for the V=O groups was present at 947 cm^{-1} for **1** and 968 cm^{-1} for **2**. The described tentative assignments are in agreement with those previously reported in dinuclear V(V)-peroxo complexes[25,28,34−36] and consistent with infrared frequencies previously attributed to carboxylate-containing ligands bound to different metal ions.[37]

Raman Spectroscopy. Complex **1** was characterized by Raman microscopy. Raman spectroscopy has already been successfully utilized to characterize vanadium peroxo complexes.[38−42] Typical bands assigned to V=O, $V-O_p$ (peroxo), and O−O vibrations in V(V)-peroxo complexes[40−42] are observed in the spectral windows of 920−1000, 660−440, and 800−940 cm^{-1}, respectively. In the Raman spectra of **1** shown in Figure 4 either in the full vibrational window or in the low-frequency part (shown in the inset), the strong scattering peak at 947 cm^{-1} and the Raman band of medium scattering intensity at 884 cm^{-1} are attributed to the V=O and O−O stretching vibrations, respectively. Similar Raman bands had been observed before for a phosphate-bridged dinuclear peroxovanadate species.[43] The Raman bands located at 637 (ν_1), 594 (ν_2), 508 (ν_3), and 462 (ν_4) are

(20) Szentivanyi, H.; Stomberg, R. *Acta Chem. Scand. A* **1984**, *38*, 101–107.
(21) Stomberg, R.; Olson, S.; Svensson, I.-B. *Acta Chem. Scand. A* **1984**, *38*, 653–656.
(22) Stomberg, R.; Svensson, I.-B. *Acta Chem. Scand.* **1971**, *25*, 898–910.
(23) Lapshin, A. E.; Smolin, Y. I.; Shepelev, Y. F.; Gyepesova, D.; Schwendt, P. *Acta Crystallogr.* **1989**, *C45*, 1477–1479.
(24) Suchá, V.; Sivák, M.; Tyršelová, J.; Marek, J. *Polyhedron* **1997**, *16*, 2837–2842.
(25) Kaliva, M.; Raptopoulou, C. P.; Terzis, A.; Salifoglou, A. *Inorg. Chem.* **2004**, *43*, 2895–2905.
(26) Tsaramyrsi, M.; Kavousanaki, D.; Raptopoulou, C. P.; Terzis, A.; Salifoglou, A. *Inorg. Chim. Acta* **2001**, *320*, 47–59.
(27) Djordjevic, C.; Lee, M.; Sinn, E. *Inorg. Chem.* **1989**, *28*, 719–723.
(28) Kaliva, M.; Giannadaki, T.; Raptopoulou, C. P.; Tangoulis, V.; Terzis, A.; Salifoglou, A. *Inorg. Chem.* **2001**, *40*, 3711–3718.
(29) Szentivanyi, H.; Stomberg, R. *Acta Chem. Scand. A* **1983**, *37*, 709.
(30) (a) Lever, A. B. P.; Gray, H. B. *Inorg. Chem.* **1980**, *19*, 1823–1824. (b) Lever, A. B. P.; Gray, H. B. *Acc. Chem. Res.* **1978**, *11*, 348–355.
(31) Evans, D. F. *J. Chem. Soc.* **1957**, 4013–4018.
(32) Bhattacharjee, M.; Chaudhuri, M. K.; Islam, N. S.; Paul, P. C. *Inorg. Chim. Acta* **1990**, *169*, 97–100.
(33) Deacon, G. B.; Philips, R. *J. Coord. Chem. Rev.* **1980**, *33*, 227–250.
(34) (a) Wright, D. W.; Humiston, P. A.; Orme-Johnson, W. H.; Davis, W. M. *Inorg. Chem.* **1995**, *34*, 4194–4197. (b) Zhou, Z.-H.; Wan, H.-L.; Tsai, K.-R. *Chin. Sci. Bull.* **1995**, *40*, 749. (c) Velayutham, M.; Varghese, B.; Subramanian, S. *Inorg. Chem.* **1998**, *37*, 1336–1340.
(35) Griffith, W. P.; Wickins, T. D. *J. Chem. Soc. A* **1968**, 397–400.
(36) Vuletic, N.; Djordjevic, C. *J. Chem. Soc., Dalton Trans.* **1973**, 1137–1141.
(37) (a) Matzapetakis, M.; Raptopoulou, C. P.; Terzis, A.; Lakatos, A.; Kiss, T.; Salifoglou, A. *Inorg. Chem.* **1999**, *38*, 618–619. (b) Matzapetakis, M.; Raptopoulou, C. P.; Tsohos, A.; Papefthymiou, B.; Moon, N.; Salifoglou, A. *J. Am. Chem. Soc.* **1998**, *120*, 13266–13267. (c) Matzapetakis, M.; Dakanali, M.; Raptopoulou, C. P.; Tangoulis, V.; Terzis, A.; Moon, N.; Giapintzakis, J.; Salifoglou, A. *J. Biol Inorg. Chem.* **2000**, *5*, 469–474. (d) Matzapetakis, M.; Karligiano, N.; Bino, A.; Dakanali, M.; Raptopoulou, C. P.; Tangoulis, V.; Terzis, A.; Giapintzakis, J.; Salifoglou, A. *Inorg. Chem.* **2000**, *39*, 4044–4051. (e) Matzapetakis, M.; Kourgiantakis, M.; Dakanali, M.; Raptopoulou, C. P.; Terzis, A.; Lakatos, A.; Kiss, T.; Banyai, I.; Iordanidis, L.; Mavromoustakos, T.; Salifoglou, A. *Inorg. Chem.* **2001**, *40*, 1734–1744.
(38) Schwendt, P.; Volka, K.; Suchánek, M. *Spectrochim. Acta* **1988**, *44A*, 839–844.
(39) Campbell, N. J.; Dengel, A. C.; Griffith, W. P. *Polyhedron* **1989**, *8*, 1379–1386.
(40) Schwendt, P.; Sivak, M.; Lapshin, A. E.; Smolin, Y. I.; Shepelev, Y. F.; Gyepesova, D. *Transition Met. Chem.* **1994**, *19*, 34–36.
(41) Schwendt, P.; Tyrselova, J.; Pavelcik, F. *Inorg. Chem.* **1995**, *34*, 1964–1966.
(42) Kozlov, A.; Kozlova, A.; Asakura, K.; Iwasawa, Y. *J. Mol. Catal. A: Chem.* **1999**, *137*, 223–237.
(43) Rosado, M. T.; Duarte, M. L. T. S.; Fausto, R. *Vib. Spectrosc.* **1998**, *16*, 35–54.

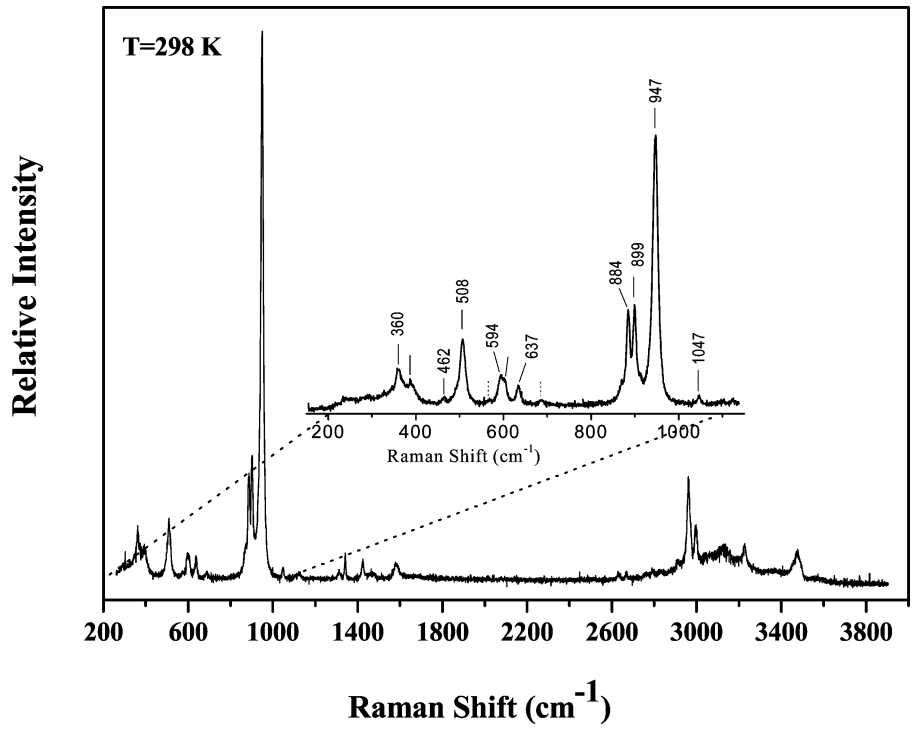

Figure 4. Raman spectrum of **1** in the solid state. Excitation with a visible laser line at 514.5 nm. Inset: Raman spectrum of the low frequency part with a $\lambda/4$ positioned between the focusing objective lens and the sample.

attributed to the four V−O_p stretching modes. The Raman frequencies of the four V-O_p normal modes for mononuclear complexes[40] and the position of the more intense ν_3 (V-O_p) stretching mode for dinuclear[43] diperoxo complexes provided the opportunity to reveal the coordination number of the V(V) ions. In this work, either through the increased shift between the ν_1 and the ν_2 V−O_p stretching vibration or the low-frequency position of the stronger ν_3 (V−O_p) stretching vibration, a pentagonal bipyramidal arrangement around vanadium ions with an apical V−O bond of 2.36 Å is expected. This rather large V−O distance is closely comparable with the corresponding 2.328(3) Å (V(1)−O(7)) and 2.354(3) Å (V(2)−O(3)) distances given by the X-ray crystallographic analysis. Moreover, the Raman band at 899 cm^{-1} is tentatively attributed to a C−C and C−N stretching of the zwitterionic form of glycine, while the low intensity Raman peaks at 1047 and 360 cm^{-1} are attributed to C−C−N antisymmetric stretching and bending modes, respectively.[43]

Solid State NMR Spectroscopy. The ^{13}C CP-MAS NMR spectrum of **1** (Figure 5A) was consistent with the coordination mode of the glycinate ligand around the V(V) ion. The spectrum exhibits two distinct peak resonances. One of those lies in the high field region, whereas the other one emerges in the low field region. The peak in the high field region at 43.9 ppm could be assigned to the methylene carbon located adjacent to the coordinated carboxylate of the bound glycinate ligand. In the low field region, where the carbonyl carbon resonance is expected to appear, there was a resonance at 179.3 ppm for the glycinate carboxylate group, bound to the two V(V) ions of the central core. These observations were subsequently confirmed by X-ray crystallography.

Solution NMR Spectroscopy. The solution ^{13}C NMR spectrum of complex **1**was measured in D_2O (Figure 5B). The spectrum revealed the presence of two resonances. The resonance in the high field region (44.3 ppm) was attributed to the CH_2 group of the glycinate ligand bound to the central V(V) ion of the dinuclear core. The signal at 175.1 ppm in the lower field region was assigned to the carbon of the carboxylate group coordinated to the V(V) ion. These signals were shifted to lower fields in comparison to the resonances in pure glycine. The shift was ∼3.0 ppm downfield and was comparable to that observed in the ^{13}C CP-MAS solid-state NMR spectrum of **1**. It is worth noting that the pattern of resonances observed was similar to that observed in the solid-state ^{13}C CP-MAS NMR spectrum of **1**. The ^1H NMR spectrum of **1** in D_2O showed one peak at 3.4 ppm consistent with the presence of the methylene protons on the glycinate ligand bound to V(V). A very small downfield shift of the proton resonance was also observed in this case compared to pure glycine. Overall, there was a consistency between the solid and solution state spectra.

Cyclic Voltammetry. The cyclic voltammetry of complex **1** was studied in aqueous solutions, in the presence of KNO_3 as a supporting electrolyte. The cyclic voltammogram exhibits ill-defined electrochemical waves reflecting (a) a reduction wave at $E_{pc} = -1.0$ V, and (b) an oxidation wave at $E_{pa} = -0.7$ V ($\Delta E = 300$ mV, $ip_a/ip_c < 1$, $ip_c/\{(v)^{1/2}C\}$ variable). This voltammetric behavior projects irreversible V^V/V^{IV} redox processes associated with species **1**. The observed irreversibility is not easily understood at the present time as it might involve complex processes encompassing concurrent oxidation state and coordination number changes associated with the presence/absence of peroxide on the V_2O_2

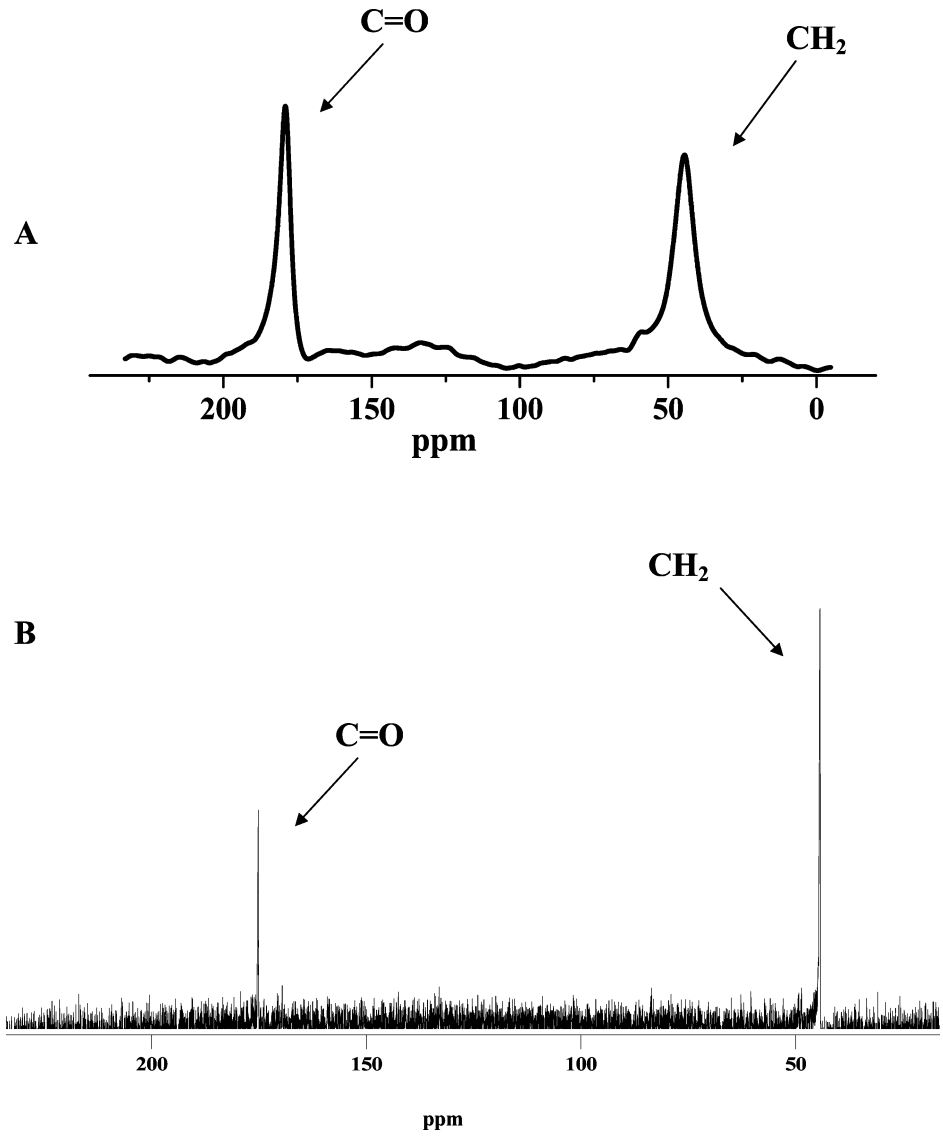

Figure 5. CP-MAS ^{13}C NMR spectrum of complex **1** in the solid state (**A**) and ^{13}C NMR spectrum of **1** in solution (**B**).

Scheme 1

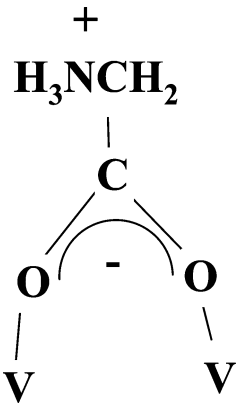

core. Attempts to pursue the isolation of reduced products **1** and **2** are currently ongoing.

Discussion

Ternary V(V)-Peroxo-Amino Acid Chemistry. The propensity of vanadium to promote binary and ternary interactions has been exploited, in the past decade, to synthesize compounds capable of (a) participating in catalytic transformations[44] of small molecules, and (b) exhibiting insulin mimetic or antitumorigenic activities in biologically relevant media. In both cases, one of the outstanding features emerging as a common factor was the presence of peroxo moieties bound to vanadium(V). Consequently, the chemistry of binary V(V)-peroxo and ternary V(V)-peroxo-L (L = low or high molecular mass cellular target) compounds was avidly pursued providing a number of species, which were isolated in the solid state and characterized crystallographically. Such V(V)-peroxide species[45] were shown to exhibit insulin mimetic activity in vitro.

(44) (a) Conte, V.; Di Furia, F.; Lucini, G. *Appl. Catal., A* **1997**, *157*, 335–361. (b) Kadena, K.; Kawanishi, Y.; Jitsukawa, K.; Teranishi, S. *Tetrahedron Lett.* **1983**, *45*, 5009. (c) Edwards, J. O.; Curci, R.: In *Catalytic Oxidations with Hydrogen Peroxide as Oxidant*; Strukul, G., Ed.; Kluwer Academic Publishers: Dordrecht, 1992; p 97. (d) Bortolini, O.; Conte, V. *J. Inorg. Biochem.* **2005**, *99*, 1549–1557.

(45) Shaver, A.; Hall, D. A.; Ng, J. B.; Lebuis, A.-M.; Hnes, R. C.; Posner, B. I. *Inorg. Chim. Acta* **1995**, *229*, 253–260.

In view of (a) the chemical affinity of vanadium(V) for peroxide moieties,[46] (b) the diverse structural chemistry of vanadium with peroxides, and (c) the ability of vanadium(V) to form both mono- and diperoxo binary as well as ternary complexes with physiological or biomimetic ligands, it emerged as a challenge to investigate the chemistry of vanadium(V) with hydrogen peroxide in the presence of carboxylate-bearing substrates. Among such ligands was the simplest of amino acids, that is, glycine. The synthetic procedure employing the simple reagents V_2O_5, glycine, and hydrogen peroxide, under carefully tuned pH conditions, led to the isolation of the rare complexes **1** and **2** in an expedient fashion. The synthetic process, under specific pH and molecular stoichiometry, unraveled specific structural and chemical attributes for **1** and **2**, as well as species arising from other V(V)-peroxo-L systems, with L being organic O- and N-containing physiological or biomimetic substrates.[47] The results of the physicochemical characterization of **1** and **2** in the solid state and in solution through elemental analysis, LC-MS (**2**), multinuclear NMR in the solid state and in solution, FT-IR, Raman, and cyclic voltammetry were in line with the crystallographic structures of those species and projected well-defined species emerging from aqueous media.

Rare Ternary V(V)-Peroxo-Amino Acid Species. The chemical reactivity of the ternary V(V)-peroxo-glycine system led to the rarely encountered anions in **1** and **2**. In both cases, two peroxo moieties were concurrently attached to V(V), with two such V(V) units joined through peroxide terminal interactions giving rise to a dinuclear assembly. Key points in these unusual species include the following.

(a) The involvement of base in the reaction (ammonia vs potassium hydroxide). Both ammonia and potassium hydroxide were used as bases to adjust the pH of the reaction mixture yet ammonia did not enter the solid state lattice (in the form of ammonium cation), within which complex **1** was isolated. That fact was also supported by elemental analysis. Hydronium ions, instead, were present in the lattice and stabilized the arisen anionic dinuclear species. In numerous other occasions of ternary dinuclear V(V)-peroxo-hydroxycarboxylate species, employment of inorganic bases in the synthesis reaction mixtures had led to the incorporation of the requisite inorganic cations (generated by the base) in the lattice of the isolated compound.[25−28] When KOH was used, the potassium ion fitted appropriately into the lattice of **2**, effectively balancing out the negative charge of the dinuclear assembly. It appears, therefore, that regardless of the base-derived countercation, the anionic assembly $[V_2(O)_2(\mu_2{:}\eta^2{:}\eta^1\text{-}O_2)_2(\eta^2\text{-}O_2)_2(C_2H_5NO_2)]^{2-}$ stays intact in **1** and **2**.

(b) The nature of amino acid glycine coordinated to V(V). It appears that glycinate adopts a zwitterionic form and as such it is bound to V(V) through the anionic carboxylate group. It is very likely that the presence of the zwitterionic glycinate ligand contributes to the stability of the dinuclear divanadium-tetraperoxo core in **1** and **2**.

(c) The mode of coordination of the glycinate ligand to the dinuclear assembly. Glycinate inserts itself into the dinuclear core through the carboxylate group in a bidentate fashion, acting as a bimetallic center bridge and essentially locking the interaction in place.

Structural comparison of **1** and **2** with other V(V)-diperoxo species reveals striking similarities and differences in the structure of the $[(V^V{=}O)(O_2)_2]_2^{2-}$ dinuclear core assembly, hosting bridging ligands, varying from O^{2-} to carboxylate-bearing linkers. To this end, in the case of $(NH_4)_4[O\{VO(O_2)_2\}_2]$, the tetraperoxodivanadate anion $[O(VO(O_2)_2)_2]^{4-}$ can be described as being composed of two pentagonal bipyramids sharing faces. In this assembly, as the two V(V) bipyramids draw closer to each other, the two vanadium units bend so as to accommodate a more compact structure. In that respect, the O^{2-} bridge plays an important role in rendering the coordination geometry around each vanadium ion pentagonal bipyramidal. Quite analogous is the case of the anion $[V_2O_2(O_2)_4(H_2O)]^{2-}$.[23,24] In the case of the $[H\{VO(O_2)_2bipy\}_2]^-$ ions in $(Hbipy)[H\{VO(O_2)_2(bipy)\}_2]\cdot xH_2O_2\cdot(6-x)H_2O$ ($x \sim 0.5$),[20] the peroxo oxygens and one nitrogen anchor from the 2,2′-bipyridine ligand lie in a pentagonal equatorial plane, while the vanadyl oxygen atom and the other nitrogen atom occupy the axial positions. In the assembled dinuclear complex, the two $[VO(O_2)_2(bipy)]^-$ moieties, which are related by an inversion center, are held together through a fairly strong hydrogen bond, with the O−H···O distance being 2.456(4) Å. On the basis of the structural description, the complex differs from the dinuclear $[O\{VO(O_2)_2\}_2]^{4-}$, previously dwelled on, in which the two vanadium(V) ions are linked through an oxygen O^{2-} bridge. In the case of the anion in **1** and **2**, it appears that the basic divanadium tetraperoxo core retains its $[(V^V{=}O)(O_2)_2]^-$ identity upon coordination of the zwitterionic glycinate. The latter ligand essentially (a) dictates the V···V distance between the two $[(V{=}O)(O_2)_2]^-$ units in the tetranuclear assembly. The distances are 3.372(2) (**1**) and 3.381(4) (**2**) Å and appear to be longer than the ones observed in $[O(VO(O_2)_2)_2]^{4-}$ (3.044(6) Å),[22] $[V_2O_2(O_2)_4(H_2O)]^{2-}$ (3.120 Å),[23] and $[V_2O_2(O_2)_4(H_2O)]^{2-}$ (3.239(5) Å).[24] The observed increase in V···V distance from the aforementioned species to the anions in **1** and **2** may be attributed to the span of the carboxylate oxygens of the glycinate moiety as the latter coordinates to the core assembly, and (b) brings the two units closer to each other compared to the species mentioned above. In this sense, the mode of coordination of the amino acid zwitterion is worth paying attention to. The acetate group of glycinate binds in a $\eta^1,\eta^1{:}\mu_2$ fashion to the dinuclear vanadium assembly: (a) acting as a bidentate bridging linker, (b) sustaining the tetraperoxo framework, and (c) very likely bestowing stability to the tetraperoxo core (Scheme 1).

As for the NH_3^+ group of the zwitterionic amino acid, it plays a significant role, in view of (a) its positive charge and the presence of hydrogens attached to the nitrogen

(46) (a) Einstein, F. W. B.; Batchelor, R. J.; Angus-Dunne, S. J.; Tracey, A. S. *Inorg. Chem.* **1996**, *35*, 1680. (b) Begin, D.; Einstein, W. B.; Field, J. *Inorg. Chem.* **1975**, *14*, 1785.

(47) (a) Kaliva, M.; Gabriel, C.; Raptopoulou, C. P.; Terzis, A.; Salifoglou, A. *Inorg. Chim. Acta* **2008**, *361*, 2631–2640. (b) Kaliva, M.; Kyriakakis, E.; Gabriel, C.; Raptopoulou, C. P.; Terzis, A.; Tuchagues, J.-P.; Salifoglou, A. *Inorg. Chim. Acta* **2006**, *359*, 4535–4548.

terminal, and (b) its proximity to oxygen terminals belonging to vanadium-bound peroxo moieties. That role is exemplified in the process of packing and the ensuing assembly of the lattice of **1** and **2**. In complex **1**, the NH_3^+ group participates in the formation of H-bonds with O anchors belonging to the peroxide groups bound to the vanadium ions in the *bc* plane (along the *a* axis). Specifically, along the *b* axis, H-bonds emerge between O(5) and H1A (O5···H1A 1.997(3) Å), with O(5) belonging to the peroxide group bound to V(1), and H1A originating in the NH_3^+ group of an adjacently located V(V)-peroxo-glycinate complex. Along the *c* axis, H-bonds appear between O(8) and H1C (O8···H1C 2.453(3) Å), where O(8) belongs to the peroxide group bound to V(2), and H1C belongs to the NH_3^+ group of the neighboring tetraperoxo vanadium core. In complex **2**, the NH_3^+ group in the *ab* plane (along the *c* axis) participates in the formation of H-bonds with O terminals from peroxide moieties bound to vanadium ions. Specifically, the H-bonds emerge between O(7) and H1C (O7···H1C 1.954(5) Å), with O(7) belonging to the peroxide group bound to V(2) and H1C belonging to the NH_3^+ group of the neighboring tetraperoxo core. Undoubtedly, therefore, the NH_3^+ group plays a distinct and essential role in the formation of a variable number of hydrogen bonds and in so doing it contributes to the packing and stability of the respective lattices in **1** and **2**.

Worth noting in the lattice of **2** are structural features projecting the existence of elliptical cavities defined by the pentagonal bipyramidal vanadium(V) and nine-coordinate potassium units traversing the unit cell in the specific directions. To that end, the packing diagram of **2** in the *ac* plane (Figure 2A) shows an ellipsoid with dimensions d_1 7.666 Å (*a* axis length) and d_2 3.857 Å, and a surface of 23.2 $Å^2$. Formation of a 12 member cyclic ring encompassing four vanadium ions and two potassium assemblies supports such an opening in the lattice structure of **2**. The elliptical void extends deep into the lattice along the *b* axis, projecting a unit volume of 184.5 $Å^3$. In the same lattice, displayed in the packing diagram of **2** off the *abc* diagonal (Figure 2B), another elliptical void appears with dimensions d_1 7.953 Å (*b* axis length) and d_2 11.792 Å (*c* axis length), and a surface of 73.49 $Å^2$. A 16 member cyclic ring assembled upon joining four vanadium and four potassium units formulates the elliptical size of this gap. The unit volume for the elliptical channel along the third dimension rises to 283.5 $Å^3$. The aforementioned elliptical cavities run simultaneously in two different directions inside the lattice of **2**, thus projecting the structural fingerprint of the requisite lattice. No such clear-cut structural features were observed in the case of **1**.

Potential Linkage to V(V)-Peroxo Mimesis or Influence of Cellular Processes. Vanadium(V)-peroxo complexes of the type $M_x[V(=O)(O_2)L]$ and $M_x[V(=O)(O_2)_2L]$ (where **L** is an appropriate organic vanadium binder and *x* is a function of the charge of L) have been shown to exert insulin mimetic activity in *in vitro* and *in vivo* experiments.[48] In fact, the triggering and often stimulating activity of peroxovanadates toward biochemical processes, such as protein tyrosine phosphorylation and protein tyrosyl phosphatase activity relating to insulin mimesis, has been shown to be more potent (at least 4-fold) than that exhibited by the non-peroxo vanadate compounds.[8] Beyond this, peroxovanadates have been shown to act in homogeneous catalysis,[49] as possible models in the mechanism of vanadium haloperoxidase,[50] and even further as species displaying antitumor activity.[5] The latter action by vanadium peroxides has been linked to the presence of V(V)-diperoxo species and even more so to dinuclear vanadium tetraperoxo compounds.[51] In the present case, the title complexes **1** and **2** bear the fundamental characteristics of species shown to exhibit such activity, that is, diperoxo vanadium units, in a tetraperoxo assembly. As a matter of fact, in line with previously mentioned characteristic features of antitumor displaying activity V(V)-peroxo species versus non-peroxo vanadium species in biologically relevant media, complexes **1** and **2** possess among others: (a) a seven-coordinate V(V) in a pentagonal bipyramidal geometry and the peroxo groups in a position *cis* to the V=O moiety, (b) a long V−O bond *trans* to the V=O moiety (2.328(3) vs 1.609(2) Å and 2.354(3) vs 1.617(2) Å in **1**, and 2.378(3) vs 1.609(3)Å and 2.346(3) vs 1.609(3) Å in **2**). Concurrently, there is another striking difference between the herein described species and the previously reported divanadium tetraperoxo complexes, namely, the presence of a biologically important substrate, that is, the amino acid glycinate. Glycinate presence in the anions of **1** and **2** may, as a result of the chemistry involved, reflect modulation of the chemical reactivity of vanadium-peroxo species, which in turn diversify their biochemical action in cellular media. Hence, it remains to be seen whether or not (a) other amino acid (e.g., glutamic, aspartic, etc.) derivatives of the same or similar V(V)-peroxo structure can be synthesized, isolated, and characterized, and (b) amino acid bound V(V)-diperoxo-containing units exhibit biological activity (e.g., in insulin mimesis or antitumorigenesis) differentially distinct from their amino acid free counterparts already known in the literature for their chemical and biological activity.

In view of the pluripotent chemical reactivity of vanadium peroxides, the fundamental $[(V^V=O)(O_2)_2]^-$ units (a) are generated in aqueous media, (b) persist in aqueous media, (c) bear bound physiological heteroligands such as amino acids (i.e., glycinate) in a zwitterionic form, and (d) are poised to reflect a chemical propensity toward cellular targets and processes influencing the physiology/pathology of cells. It remains to be seen whether the herein unusual dinuclear V(V)-tetraperoxo species will influence cellular events in vitro or in vivo.

(48) Shaver, A.; Ng, J. B.; Hall, D. A.; Loon, B. S.; Posner, B. I. *Inorg. Chem.* **1993**, *32*, 3109.

(49) (a) Di Furia, F.; Modena, G. *Rev. Chem. Intermed.* **1985**, *6*, 51. (b) Köpf-Maier, P.; Wagner, W.; Hesse, B.; Köpf, H. *Eur. J. Cancer* **1981**, *17*, 665.

(50) (a) Djordjevic, C.; Lee, M.; Jacobs, B. A.; Puryear, B. C. *J. Inorg. Biochem.* **1989**, *36*, 239. (b) Wever, R.; Kustin, K. *Advances in Inorganic Chemistry: Vanadium, a Biologically Relevant Element*; Sykes, A. G., Ed.; Academic Press, Inc.: New York, 1990; Vol. *35*, p 81.

(51) Cundari, T. R.; Zerner, M. C.; Drago, R. S. *Inorg. Chem.* **1988**, *27*, 4239.

Conclusions

An unusual family of ternary dinuclear vanadium-(di)peroxo-glycine species was synthesized, isolated (in the presence of different cations), and characterized in the solid state and in solution. The structural features are distinct from those of simple vanadium-diperoxo species, which themselves are very few. The dinuclear nature of vanadium-diperoxo moieties does not deviate significantly from the one known thus far. The presence of amino acid glycinate as a zwitterion likely contributes to the solubility and stability of the existing species. Given that these species bear a physiologically important moiety present in human fluids, it would be important to investigate whether glycinate-bearing V(V)-peroxo species exhibit biological activity, in line with previously observed activity shown by ternary V(V)-peroxo-L species. In view of this advancement in vanadium-peroxo chemistry, it would be equally challenging to investigate the possibility that other amino acids, apart from glycine, may promote the same or similar chemistry to the one shown here with vanadium and hydrogen peroxide. In this regard, it would be important to see whether or not the physicochemical properties of binary vanadium-tetraperoxo species interacting with amino acids can be modulated (e.g., through pH-dependent synthesis) providing finely tuned soluble and potentially bioavailable forms of vanadium, capable of promoting further interactions with higher molecular mass biomolecules. Such ternary interactions, covering a wide spectrum of vanadium reactivity, could contribute to triggering critical events in signal transduction pathways linked to insulin mimesis or antitumorigenesis. The chemistries associated with such interactions are currently being investigated in our laboratory.

Acknowledgment. The authors would like to acknowledge the financial support to this project by a "PENED" grant co-financed by the E.U.-European Social Fund (75%) and the Greek Ministry of Development-GSRT (25%).

Supporting Information Available: CIF files of X-ray crystal structure refinement data for $(H_3O)_2[V_2(O)_2(\mu_2{:}\eta^2{:}\eta^1\text{-}O_2)_2(\eta^2\text{-}O_2)_2(C_2H_5NO_2)]\cdot 5/4H_2O$ (**1**) and $K_2[V_2(O)_2(\mu_2{:}\eta^2{:}\eta^1\text{-}O_2)_2(\eta^2\text{-}O_2)_2(C_2H_5NO_2)]\cdot H_2O$ (**2**), and the ORTEP diagram of **2**. This material is available free of charge via the Internet at http://pubs.acs.org.

IC801427B